Extremophiles (2009) 13:1–10
DOI 10.1007/s00792-008-0190-6

ORIGINAL PAPER

The stability of the archaeal HU histone-like DNA-binding protein from *Thermoplasma volcanium*

Fotini Orfaniotou · Pavlos Tzamalis · Angelos Thanassoulas · Eleni Stefanidi · Athanassios Zees · Effrosini Boutou · Metaxia Vlassi · George Nounesis · Constantinos E. Vorgias

Received: 20 July 2008 / Accepted: 1 September 2008 / Published online: 26 September 2008

Abstract The complete genome analysis of the archaeon *Thermoplasma volcanium* has revealed a gene assigned to encode the histone-like DNA-binding protein HU. *Thermoplasma volcanium* is a moderate thermophile growing around 60°C and it is adaptable to aerobic and anaerobic environment and therefore it is unique as a candidate for the origin of eukaryotic nuclei in the endosymbiosis hypothesis. The HU protein is the major component of the bacterial nuclei and therefore it is an important protein to be studied. The gene for HU*Tvo* protein (*huptvo*) was cloned from the genomic DNA of *T. volcanium* and over-expressed in *Escherichia coli*. A fast and efficient purification scheme was established to produce an adequate amount of bioactive protein for biochemical and biophysical studies. Highly purified HU*Tvo* was studied for its DNA-binding activity and thermostability. As studied by circular dichroism and high-precision differential scanning microcalorimetry, the thermal unfolding of HU*Tvo* protein is reversible and can be well described by a two-state model with dissociation of the native dimeric state into denatured monomers. The ΔG versus T profile for HU*Tvo* compared to the hyperthermophilic marine eubacterial counterpart from *Thermotoga maritima*, HU*Tmar*, clearly shows that the archaeal protein has adopted a less efficient molecular mechanism to cope with high temperature. The molecular basis of this phenomenon is discussed.

Keywords Archaea · *Thermoplasma volcanium* · DNA-binding protein HU · Cloning · Purification · Thermodynamic stability · Thermal unfolding

F. Orfaniotou and P. Tzamalis contributed equally to this work.

F. Orfaniotou · E. Stefanidi · A. Zees · E. Boutou · C. E. Vorgias (✉)
Department of Biochemistry and Molecular Biology, Faculty of Biology, National and Kapodistrian University of Athens, Panepistimiopolis-Zographou, 15784 Athens, Greece
e-mail: cvorgias@biol.uoa.gr

P. Tzamalis · A. Thanassoulas · G. Nounesis
Biomolecular Physics Laboratory, I/R-RP, National Centre for Scientific Research "Demokritos", Aghia Paraskevi, 15310 Athens, Greece

M. Vlassi
Institute of Biology, National Centre for Scientific Research "Demokritos", Aghia Paraskevi, 15310 Athens, Greece

Introduction

The bacterial cell nucleoid contains a number of low-molecular-weight basic proteins, namely the histone-like DNA-binding proteins. HU genes have been identified in over 100 bacterial genomes.

The first HU protein was isolated in *Escherichia coli* as one of the most abundant DNA-binding proteins, estimated to exist in populations of 30,000 dimers per cell. HU in *E. coli* is a heterodimer consisting of two subunits each of 90 aa (amino acid) residues. HU has been shown to be a homodimer in nearly all other bacterial species where it has been studied except in *E. coli*, *Serratia marcescens*, and *Salmonella typhimurium.* Comprehensive reviews on HU proteins have already been published (Drlica and Rouviere-Yaniv 1987; Pettijohn 1988; Oberto et al. 1994; Schmid 1990).

The HU proteins are abundant in many prokaryotes and exhibit a high sequence homology among various species (Drlica and Rouviere-Yaniv 1987). Initially, HU was described to bind to DNA in a sequence-independent manner and to assemble into supramolecular nucleoprotein

complexes (Rouvière-Yaniv et al. 1979). In archaea, based on bioinformatics, three organisms have been detected to contain genes encoding HU DNA-binding protein. These organisms are *Thermoplasma acidophilum* (Ruepp et al. 2000), *Picrophilus torridus* (Futterer et al. 2004), and *T. volcanium* (Kawashima et al. 2000).

Many published results clearly demonstrated that HU is involved in a variety of bacterial metabolic functions of DNA and regulatory events; among others, replication, transcription, transposition and repair (Lavoie and Chaconas 1994; Castaing et al. 1995; Kamashev and Rouvière-Yaniv 2000; Esser et al. 1999; Hwang and Kornberg 1992).

Several crystal structures of HU or HU/DNA complexes have been published. The first solved structure of HU was acquired from *Bacillus stearothermophilus* (HU*Bst*) (Tanaka et al. 1984) and refined at 2 Å (White et al. 1999) resolution. The solution structure of recombinant HU from *B. stearothermophilus* (Padas et al. 1992) has also been determined by NMR (Boelens et al. 1996; Vis et al. 1995). The structure of the heterodimeric form of HU from *E. coli* was also published (Coste et al. 1999).

HU protein has been extensively employed as a model system to study the structural basis of protein-DNA interaction as well as the thermal stability properties of the histone-like protein family (Christodoulou and Vorgias 2002; Christodoulou et al. 2003), in which the integration host factor (IHF) proteins also belong (Rice et al. 1996; White et al. 1989). Moreover, the application of various biophysical techniques has revealed very interesting properties of the HU proteins (Raves et al. 2001; Serban et al. 2003). Recent studies clearly support a more dynamic function of HU proteins, which was underestimated in the past (Sagi et al. 2004; Schnurr et al. 2006).

We have described the cloning and the overproduction of several HU proteins from different thermophilic and mesophilic *bacilli* (Padas et al. 1992). Recently the X-ray structure of HU protein from the extreme thermophilic marine eubacterium *T. maritima* (HU*Tmar*) was solved at high resolution (Christodoulou et al. 2003). The structural properties of HU*Tmar* in solution were also resolved by NMR and have shown an unexpected local flexibility for hyperthermophilic protein (Durney et al. 2004). The hyperthermophilic HU protein from *T. maritima* and *E. coli* have also been the subject of extensive thermodymanic analyses (Ruiz-Sanz et al. 2004).

In the present work we have extended our studies to the archaea and report the cloning of *huptvo* gene from *T. volcanium* (HU*Tvo*), the expression of the gene in *E. coli*, and the establishment of an efficient purification scheme to be able to provide adequate and suitable protein material for structural studies by X-ray crystallography and NMR. In parallel, a 3D model of HU*Tvo* was produced based on the crystal structure of HU protein from *T. maritima* and the model was subsequently used for structural comparisons. Furthermore, a comprehensive thermal stability study has been carried out and a model is proposed for the thermal unfolding pattern of the protein. Thermodynamic comparison of HU*Tvo* with HU*Tmar* has emerged as a very interesting question concerning the efficiency and mechanisms of both proteins to cope with high temperature.

Materials and methods

Materials

The enzymes used in the cloning procedures were from New England Biolabs and the pcr2.1^{TM} cloning system from InVitrogen. The column chromatography media were from Pharmacia and all the other chemicals were from Sigma or Merck (Germany), in the highest analytical grade. Synthetic oligonucleotides were prepared by VBC Genomics (Wien, Austria).

Cloning of huptvo gene

The *huptvo* gene was isolated from the genomic bacterial DNA (kindly provided by Dr. N. A. Kawashina) by gene amplification reaction (PCR). Total *T. volcanium* chromosomal DNA (1 μg) was used in a typical PCR reaction (50 μl) involving the following components at a final concentration: template DNA 20 ng/μl, *huptvo*(N) (AACA TATGGTTGGAATTAGTGAAC) that matches the 5′-end of the *huptvo* gene sequence and incorporates *Nde*I site and *huptvo*(C) (AAGGATCCTTATTGT TGGTACTTTATC) that matches the complementary strand of the 3′-end of the *huptvo* gene sequence and incorporates a stop codon before a *Bam*HI site. The gene amplification reaction was performed with the following steps per cycle: denaturation at 94°C for 1 min; annealing at 50–60°C for 1 min; and polymerisation at 72°C for 2 min. Thirty cycles were carried out using a Stratagene device and 5 μl of the amplification mixture was analysed by 1.5% agarose in TBE at 100 V constant voltage and stained with ethidium bromide (EtdBr). The amplified gene was then introduced into pcr2.1^{TM} plasmid of the TA cloning kit of InVitrogen (USA) and further verified by DNA sequencing according to the dideoxy-chain termination method (Sanger et al. 1977).

The final cloning of the *huptvo* gene for protein overproduction was carried out as described in our previous publications (Padas et al. 1992; Christodoulou et al. 2003) and following the current cloning procedures described in Sambrook et al. (1989). The resulting construct, namely pCV*huptvo*, was verified by sequencing using the primer

extension method (Sanger et al. 1977). The pCV*huptvo* expression vector was then introduced into the BLR(DE3) expression host cells (Novagen). The clone pET-11a-*huptvo*-BLR(DE3) was grown in LB medium.

Overproduction and purification of recombinant HU*Tvo* protein

HU*Tvo* protein was overproduced and purified to homogeneity based on the procedure developed and described previously (Padas et al. 1992; Christodoulou et al. 2003). Briefly, in a routine protein preparation, 1 l at $OD_{600\ nm}$ 0.8 cell culture induced with 0.5 mM IPTG at 37°C for 3 h was used. The induced bacteria were collected by low-speed centrifugation and washed once with ice cold buffer W: 50 mM Tris–HCl pH 7.5, 100 NaCl, 0.1 mM phenylmethanesulphonyl fluoride (PMSF). All further procedures were carried out at 4°C, unless otherwise specified. The bacterial paste was then re-suspended in 10 ml buffer A (20 mM Na-phosphate pH 8.0, 1 mM EDTA, 0.1 mM PMSF, 20 mM NaCl, 0.1% (w/v) Triton X-100) per gram bacterial paste. The cells were disrupted by sonication for 10 min. The total extract was then clarified by centrifugation in a Sorvall SS-34 rotor at 20,000 r.p.m. for 20 min. The supernatant was adjusted to 40% saturation in ammonium sulphate. After 30 min stirring, the non-precipitated material was separated by centrifugation as mentioned earlier. The soluble supernatant was diluted with ten volumes of buffer B (20 mM Na-phosphate, pH 8.0, 1 mM EDTA) and directly applied on a 5 ml Heparin-Sepharose CL-6B column. Bound proteins were eluted with a 0–2.5 M NaCl linear ascending gradient. Collected fractions were analysed by sodium dodecylsulphate polyacrylamide gel electrophoresis (0.1%SDS–17%PAGE). HU*Tvo* fractions were combined and diluted 1:10 with buffer C (20 mM Na-phosphate pH 7.0, 1 mM EDTA). The pH was adjusted to 7.0 and the protein solution was applied on a SP-Sepharose High Performance column. The HU protein was eluted between 600 and 800 mM NaCl via a short linear gradient between 100 and 1,000 mM NaCl. The final step provides a highly pure and concentrated HU*Tvo* protein. The overall yield varies between 15 and 25 mg of highly purified HU*Tvo* protein from 1 l bacterial culture.

Thermal denaturation studies by CD spectroscopy

Circular dichroism measurements were conducted using a Jasco-715 spectropolarimeter equipped with a Peltier type cell holder (PTC-348WI), which allows for temperature control. Wavelength scans in the far-UV region (190–260 nm) were performed in Quartz SUPRASIL (HELLMA) precision cells of 0.1 cm path length. Each spectrum was obtained by averaging five to ten successive accumulations with a wavelength step of 0.2 nm at a rate of 50 nm/min response time 2 s and band width 1 nm. Thermal CD experiments have been carried out in the range of 10–70°C, at 220 nm and heating scan rate 1.5 K/min.

Thermal denaturation studies by high-precision DSC

Calorimetric measurements were performed on a VP-DSC microcalorimeter (Microcal, USA) at a heating rate of 1.5 K/min using protein concentrations within the range 0.058–0.166 mM. The salt concentration of all the samples was low (0.1 M NaCl) and the pH was neutral (pH 7.0). All samples were scanned twice and the reproducibility of the scans showed that the denaturation was reversible under the chosen experimental conditions. To correct the experimental data, for the small error introduced by the slight differences of the two cells, the instrumental base-line determined with buffer in both cells was subtracted. A second base-line subtraction eliminated the ΔC_p which is the difference in the heat capacity between the denatured and the native state. The DSC traces were then subject to fitting procedure using ORIGIN 5.0 software from Microcal. User-designed procedures were also used.

Based on the equilibrium-analysis of the reversible calorimetric data, the stability curve can be constructed. It is represented by the temperature dependence of the change in the Gibbs free energy for the unfolding to the thermally denatured state (Ruiz-Sanz et al. 2004):

$$\Delta G(T) = \Delta H\left(1 - \frac{1}{T_{1/2}}\right) + \Delta C_p \times \left(T - T_{1/2} - T\ln\frac{T}{T_{1/2}}\right) - RT_{1/2}\ln C_T$$

Here $T_{1/2}$ is defined as the temperature at which half of the protein molecules have been thermally denatured and ΔH is the total enthalpy change.

Protein concentration

The concentration of HU*Tvo* protein was determined using various methods (Bradford 1976; Gill and von Hippel, 1989; Pace et al. 1995; Lowry et al. 1951) as well as total amino acid analysis. Finally, we have used the equation: 1 $OD_{230\ nm}$ of HU corresponds to 0.60 mg.

Protein analysis by sodium SDS-PAGE

0.1%SDS–17%PAGE analysis was run according to the Laemmli procedure (Laemmli 1970). The gels were run at constant current of 30–40 mA at room temperature and stained with Coomassie Brilliant Blue G-250.

DNA-binding assay

The DNA-binding activity of HU*Tvo* was carried out in 6% polyacrylamide gel electrophoretic mobility shift assay (EMSA). In a typical assay 0.1 ng 250 bp ^{32}P-DNA fragment, with random sequence, was incubated with highly purified recombinant HU*Tvo* protein (0.1–10 ng) incubated for 30 min at 25°C in buffer 20 mM Na-phosphate (pH 7.0) and 50 mM NaCl, and the products were separated by electrophoresis at 120 V at 4°C in TBE buffer (pH 8.3) and visualized on X-ray film.

Molecular modelling

The three-dimensional modelling was performed using the Swiss-PdbViewer v3.7b2 program (Guex and Peitsch 1997) and the homology modelling approach. The 3D model of the dimeric form of HU*Tvo* was constructed using the crystal structure of the HU protein from the extreme thermophilic marine eubacterium *T. maritima* (RCSB code: 1B8Z) (Christodoulou et al. 2003). The initial model was subsequently subjected to energy minimisation in vacuo using a version of GROMOS force field (van Gunsteren et al. 1996) as implemented in Swiss-PdbViewer v3.7b2. Analysis of the dimer interface of both the HU*Tvo* and HU*Tmar* was performed using the protein–protein interaction server (http://www.biochem.ucl.ac.uk/bsm/PP/server/index.html) (Jones and Thornton 1996) and the produced 3D-model of dimer HU*Tvo* and the 1B8Z crystal structure as queries, respectively.

Results and discussion

Comparison of the primary structure of HU*Tmar* and HU*Tvo* proteins

The sequence of the *huptvo* gene was detected in the published genome of *T. volcanium* (Kawashima et al. 2000) deposited under accession number 13540991 or NC 0026892). The deduced amino acid sequence for the HU*Tvo* protein from the sequence of the *huptvo* gene was assigned by homology. A primary structure comparison of the hyperthermostable HU*Tmar* protein from the marine eubacterium and HU*Tvo* protein from the archaeon *T. volcanium* is shown in Fig. 1a. As shown in Fig. 1a, the sequence similarity between the two HUs is high: 53% similarity and 33% identity.

Based on the above sequence similarity and the X-ray structure of HU*Tmar* (RCSB code: 1B8Z) the model of the dimeric form of HU*Tvo* was produced (Fig. 1b) as

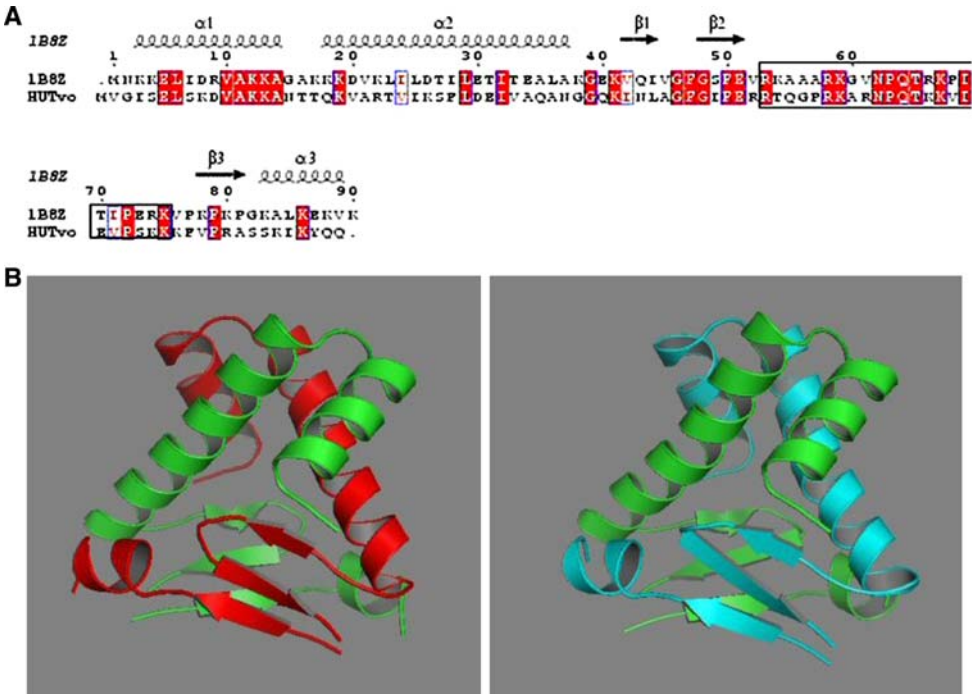

Fig. 1 **a** Sequence alignment of the thermostable HUTvo from *Thermoplasma volcanium* and HU*Tmar* from *T. maritima*. *Open* and *red-shaded boxes* correspond to similarities (according to Blosum62 matrix) and identities, respectively. Secondary structure elements on the *top row* are extracted from the crystal structure of HU*Tmar* (RCSB code:1B8Z) (Christodoulou et al. 2003). The figure was produced with the ESPrint utility (Gouet et al. 1999). **b** Ribbon representation of the dimeric form of HU*Tmar* (*left*) and HU*Tvo* (*right*) based on the 1B8Z crystal structure and the 3D-model produced in this study, respectively. Each monomer in the dimer is depicted with different *colour*. As expected by the high sequence similarity the 3D-structures of the two HUs are very similar. The figure was produced with Pymol (DeLano 2002)

described in "Materials and methods". Analysis of the dimer interface of both HU*Tvo* and HU*Tmar* showed an apolar to polar ratio of 2.3 and 2.9, respectively, whereas the total apolar to polar ratio was 0.94 and 1.1, respectively.

Overproduction and purification of HU*Tvo* protein

For protein production of HU*Tvo* protein the BLR(DE3) pCV*huptvo E. coli* cells, were used as described in "Materials and methods". Routinely, from 5 g wet cell pellet nearly 50 mg highly pure HU*Tvo* protein is obtained within 2 days (Table 1, Fig. 2).

DNA-binding activity of HU*Tvo*

The DNA-binding activity of HU*Tvo* was determined by employing EMSA. In a typical assay 0.1 ng 250 bp ^{32}P-DNA was incubated with highly purified recombinant HU*Tvo* protein in a wide range of mass ratios. The data clearly show a strong binding of HU*Tvo* to unspecific DNA and the formation of high order HU*Tvo*-DNA complexes. (Fig. 3, lanes 1–6).

Heat-induced denaturation of HU*Tvo*

The thermodynamic stability of HU*Tvo* has been determined by studying the thermally induced unfolding of the molecule via high-precision DSC and CD spectroscopy. The DSC technique accurately measures the changes of the heat capacity C_p of a dilute protein sample, at constant pressure, as the temperature is raised with an accurately controlled heating rate. At the thermal transition, non-covalent bonds are destroyed and the protein "melts" into a denatured structure-less state. In the case of HU*Tvo*, the heat-induced denaturation is a reversible process. The protein regains the native fold upon cooling.

Table 1 Purification scheme of HU*Tvo* protein from 5 g *E. coli* BLR(DE3) cells harbouring the plasmid pET-11a-*huptvo*

Step	Total amount (mg)	Yield (%)	Purification factor
Escherichia coli extract after sonication	1,350	100	1
Post 40% saturation ammonium sulphate fraction	850	63	1.6
Heparin-Sepharose column chromatography at pH 8.0, elution via 0–2.5 M NaCl gradient	60	4.4	22.5
SP-Sepharose HP column chromatography at pH 6.0; elution via 0–1 M NaCl gradient	45	3.3	30

The reversibility was tested at pH 7.0, (20 mM Na-phosphate, 100 mM NaCl buffer) at concentrations (C_t) within the range 0.058–0.166 mM, for consecutive heating DSC scans, at scan rate $u = 1.5$ K/min. Representative calorimetric data for the excess (background contributions subtracted from the original data set) heat capacity $\langle \Delta C_p \rangle$ versus temperature (T) profiles are presented in Fig. 4a for the first two consecutive DSC heating scans at $C_t = 0.149$ mM. A single endothermic peak is revealed for the thermal unfolding at $T_m \sim 56$°C (melting temperature for which $\langle \Delta C_p \rangle$ is maximum). The reversibility for the first two heating scans (estimated as the change in the total enthalpy change ΔH) varied between 88 and 93% for all the samples at various buffer solutions and concentrations that have been measured. Deviations from 100% reversibility may straightforwardly be associated with a small number of HU*Tvo* molecules that do not refold back to the native state upon cooling to room temperature. The number of these irreversibly unfolded protein molecules is directly dependent upon the total amount of time the system spends at denaturing temperatures (data not shown), which in turn

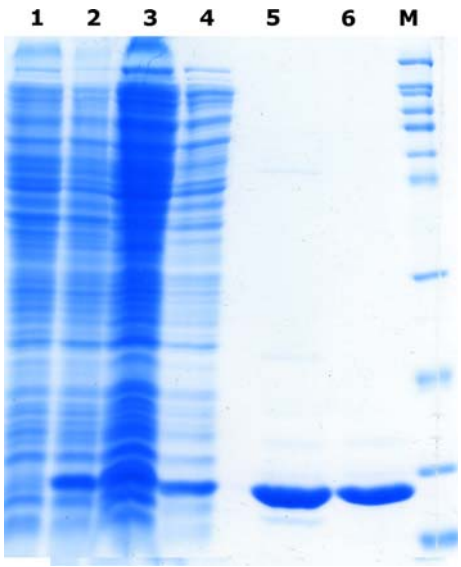

Fig. 2 0.1%SDS–17%PAGE of the major steps of the overproduction and purification of HU*Tvo*. *Lane 1* total bacterial extract of BLR(DE3) cells; *lane 2* total bacterial extract of BLR(DE3) cells harbouring the pCV*huptvo* plasmid after overnight grow in LB medium supplemented with amp and induction with 0.5 mM IPTG for 3 h; *lane 3* total soluble bacterial extract of the HU*Tvo* overproducing clone of *lane 2*; *lane 4* post 40% ammonium sulphate precipitation soluble proteins; *lane 5* peak fraction of the HU*Tvo* after elution from Heparin–Sepharose column. *Lane 6* peak fraction of HU*Tvo* after SP-Sepharose High Performance column (for details see "Materials and methods"). *Lane M* molecular weight markers from the *top*: 205 kDa: myosin, 116 kDa: beta-galactosidase, 97 kDa: phosphorylase b, 80 kDa: transferrin, 66 kDa: bovine serum albumin, 55 kDa: glutamate dehydrogenase, 45 kDa: ovalbumin, 30 kDa: carbonic anhydrase, 21 kDa: trypsin inhibitor, 14 kDa: lysozyme, 6.5 kDa: aprotinin

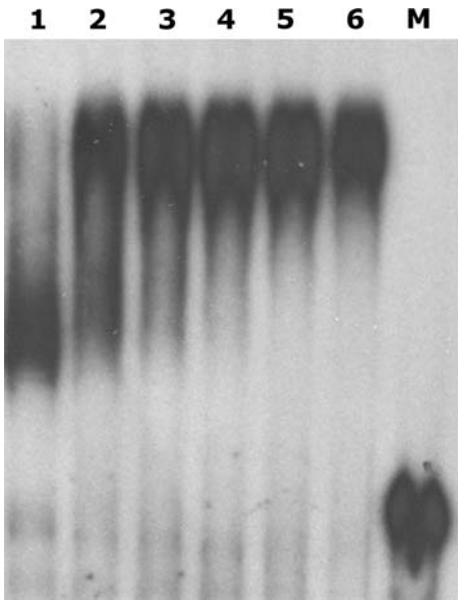

Fig. 3 Analysis of DNA–protein complexes by 6% PAGE in TBE at pH 8.3. *Lane M* 250 bp DNA, *lanes 1–6* 0.1 ng 250 bp ^{32}P-DNA complexed with 0.1, 0.5, 1.0, 2.5, 5.0 and 10 ng HU*Tvo*, respectively. Experimental details in "Materials and methods"

is indicative of the fact that the observed weak irreversibility most likely arises from the formation of small aggregates of denatured molecules. Analogous thermal transition reversibility results have been obtained from CD spectroscopy.

The heat-induced denaturation of HU*Tvo*, was also examined by directly comparing CD spectra at room temperature (20°C), in the native state, to spectra obtained at 68°C, in the denatured state and also to spectra obtained at 20°C after cooling from high temperatures. The far-UV CD spectra of HU*Tvo* at various temperatures are presented in Fig. 4b. At room temperature, the spectrum of the native state exhibits two negative CD bands at 208 and 220 nm, which are typical for $\alpha + \beta$ proteins with α and β motifs located at different domains (Damodaran 2003; Greenfield 1996). At 68°C the CD spectrum is drastically altered. It becomes very similar to characteristic spectra obtained for structure-less unfolded molecules in random-coil conformations. This drastic change is significant of extensive loss of secondary structure for the HU*Tvo* molecule in the denatured state. Indeed, analysis based on the CDNN program (Bohm et al. 1992) indicates loss of helical structure of almost 60%. However, the native spectrum is fully recovered upon cooling to room temperature confirming the reversibility of the thermal transition.

It has been established that HU proteins are either homodimeric or heterodimeric (Vis et al. 1995; Jia et al. 1996; White et al. 1999). In the high-accuracy DSC technique the dissociation of thermally unfolded oligomeric proteins into denatured monomers is manifested in the DSC profiles obtained at different sample concentrations, by a dependence of T_m upon the values of C_t. In the case of HU*Tvo*, as shown in Fig. 4c where the DSC profiles are illustrated for various samples at concentrations 0.058, 0.149, 0.160 and 0.166 mM, as well as in Table 2 where the experimental calorimetric parameters derived from these profiles are presented, such a T_m dependence is clearly observed. This is indicative of the fact that the HU*Tvo* thermograms describe the unfolding of an oligomeric protein dissociating into denatured monomers (Milardi et al. 1996).

In order to demonstrate that the thermal unfolding data obtained for HU*Tvo* describe the dissociation of HU*Tvo* dimers into denatured monomers, a more elaborate analysis was required (Manly et al. 1985; Milardi et al. 1996). By performing linear fits of the $\ln(C_t)$ versus T_m^{-1} experimental data the oligomerization index n could be obtained $n = 1.7 \pm 0.2$, which is in relatively good agreement with the initial hypothesis that native HU*Tvo* dimers dissociate during the thermal unfolding into a pair of denatured monomers ($n = 2$).

The HU protein from the hyperthermophilic eubacterium *T. maritima* exhibits analogous behaviour upon heat-induced unfolding (Ruiz-Sanz et al. 2004), dissociating into a pair of denatured monomers. On the other hand, the HU protein from *E. coli* was shown to follow a different thermodynamic path. First, it exhibits a transition into a dimeric intermediate state, which is followed at a higher temperature by the dissociation into two unfolded subunits (Ramstein et al. 2003). For the analysis of the calorimetric data that are presented here for HU*Tvo* the two-state model with dimer dissociation was applied separately for the fitting of each data set for various C_ts (Privalov and Potekhin 1986; Todd et al. 1998; Ruiz-Sanz et al. 2004).

$$N_2 \overset{K}{\leftrightarrow} 2U$$

All the results for the fitted parameters $(\Delta H)_{cal}$ (the total enthalpy change at the thermal transition and ΔC_p the heat capacity difference between the native and the denatured states) from non-linear least-squares fits are presented in Table 2. A characteristic fitted curve is displayed in Fig. 4d for the DSC profile at $C_t = 0.16$ mM. The values obtained for $(\Delta H)_{cal}$ are relatively small for a globular protein of the size of HU*Tvo*. The per-residue value of $(\Delta H)_{cal}$ is 0.38 kcal/mol residue, which is only half of the bibliographically reported value of 0.77 kcal/mol residue (Benitez-Cardosa et al. 2001). Even under the assumption that the residues participating in the flexible, already solvent-exposed DNA-binding regions have no contribution to the observed $(\Delta H)_{cal}$ and can thus be excluded from the per-residue calculation, the value of $(\Delta H)_{cal}$ increases only slightly to 0.44 kcal/mol residue, still far off from the expected. Considering that the CD

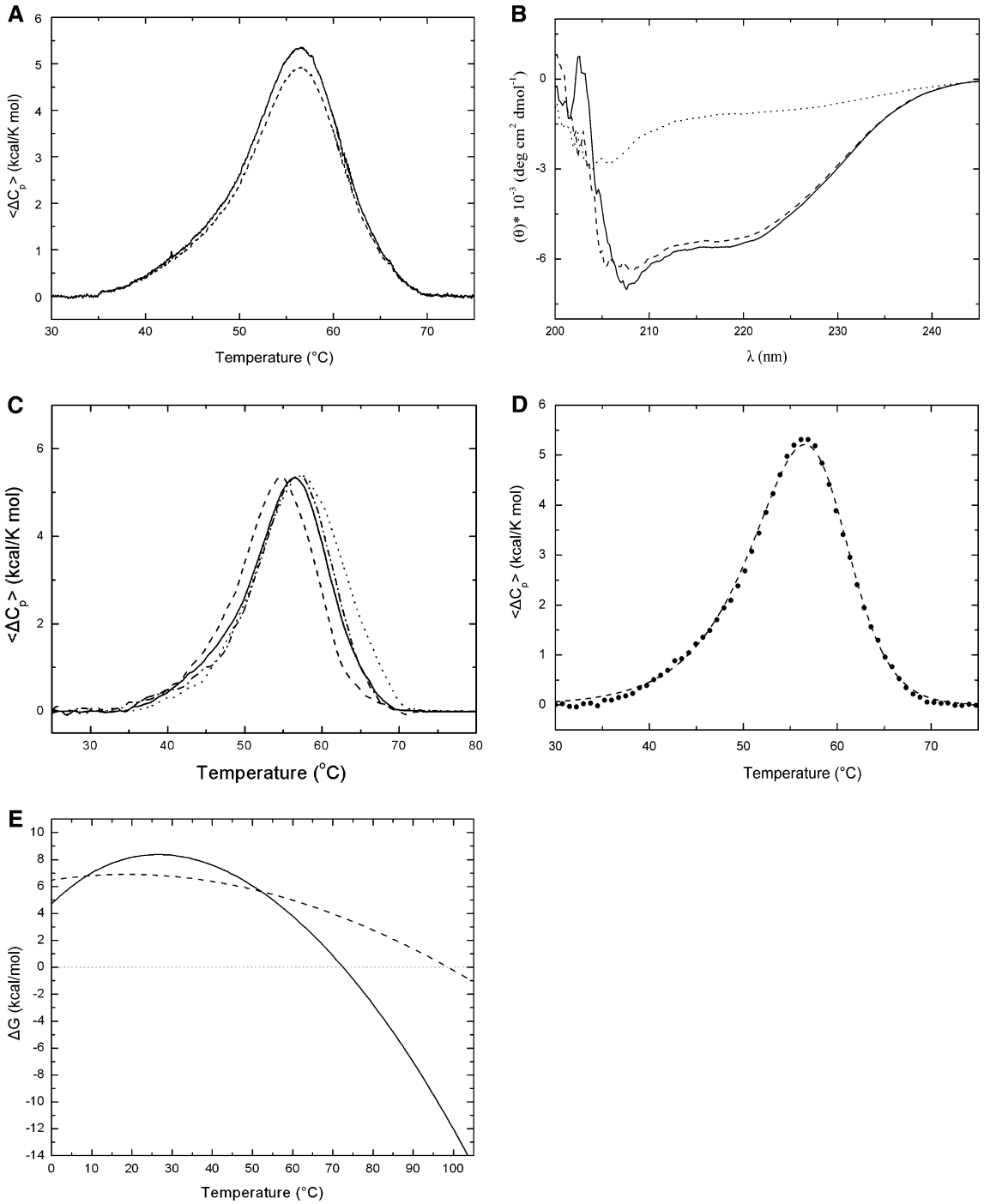

Fig. 4 **a** DSC profile for consecutive heating scans of HU*Tvo* at $C_t = 0.149$ mM, pH 7.0, (20 mM Na-phosphate, 100 mM NaCl) and heating scan rate $u = 1.5$ K/min. The *solid line* represents the first heating scan and the *dashed line* the second heating after very fast cooling to room temperature. The reversibility of the thermal unfolding is 92%. **b** Normalized far-UV CD spectra for native HU*Tvo* at 25°C (*solid line*), for the thermally denatured state at 68°C (*dotted line*) and for the refolded state after cooling from 68 to 25°C (*dashed line*). **c** $\langle \Delta C_p \rangle$ versus T profiles for the thermal unfolding of dimeric HU*Tvo*, obtained at $u = 1.5$ K/min and $C_t = 0.058$ (*dashed line*), 0.149 (*solid line*), 0.160 (*dash-dotted line*) and 0.166 mM (*dotted line*). As pointed out in the text, the dependence of T_m upon C_t is evidence for the dissociation into a pair of denatured molecules. **d** Fitting of $\langle \Delta C_p \rangle$ versus T data to the equilibrium unfolding model coupled to dimer dissociation. The *open circles* represent the $\langle \Delta C_p \rangle$ versus T trace for $u = 1.5$ K/min and $C_t = 0.45$ mg/ml. The *solid line* represents the non-linear least-squares fit. The fitting results are: $((\Delta H)_{cal})_{fit} = 72.8 \pm 3.0$ kcal/mol, $(T_m)_{fit} = 56.7 \pm 0.5$°C and $(\Delta C_p)_{fit} = 2.0 \pm 0.5$ kcal/K mol. **e** Temperature profile of the free energy change $\Delta G(T)$ from the native N to the final denatured state U of HU*Tvo*. The *dashed line* represents the results obtained for HU*Tmar* (Ruiz-Sanz et al. 2004)

Table 2 Measured and fitted parameters from analysing the DSC $\langle \Delta C_p \rangle$ versus T profiles of HU*Tvo* by a two-state with dimer dissociation model

C_t (mM)	T_m (°C)	$(\Delta H)_{cal}$ (kcal/mol)	ΔH_{vH} (kcal/mol)	$\Delta H_{vH}/(\Delta H)_{cal}$	$(T_m)_{fit}$ (°C)	$((\Delta H)_{cal})_{fit}$ (kcal/mol)
0.166	57.1 ± 0.5	71.1 ± 5.0	52.9 ± 3.7	0.74	57.0 ± 0.2	74.3 ± 2.0
0.160	56.7 ± 0.5	70.9 ± 5.0	56.0 ± 4.0	0.79	57.6 ± 0.4	72.8 ± 3.0
0.149	56.5 ± 0.5	71.4 ± 5.0	54.3 ± 3.8	0.76	56.6 ± 0.3	73.5 ± 2.0
0.058	54.8 ± 0.5	69.1 ± 3.0	49.8 ± 2.1	0.72	55.0 ± 0.3	71.1 ± 2.0

measurements reveal extensive structural changes going from the native to the denatured state, the small value of $(\Delta H)_{cal}$ is rather surprising. It is likely that since HU*Tvo* is a compact protein, total loss of the secondary structure may not necessarily be significant that all non-covalent bonds have been destroyed in the denatured state and that the structure-less molecule retains to some degree the compactness of the native fold.

Based on the equilibrium-analysis of the reversible calorimetric data, the stability curve for the HU*Tvo* protein can be constructed. It is represented by the temperature dependence of the change in the Gibbs free energy for the unfolding to the thermally denatured state (Ruiz-Sanz et al. 2004) ($\Delta G(T)$); It is plotted in Fig. 4e, at $T = 25$°C, $\Delta G = 8.4$ kcal/mol. In addition to the HU*Tvo* results, Fig. 4e illustrates the $\Delta G(T)$ profile already obtained for HU*Tmar* (Ruiz-Sanz et al. 2004) at pH 4.0, in order to facilitate direct comparisons of the thermodynamic behaviour between the two structurally similar molecules. It can straightforwardly be observed that while HU*Tvo* has a higher ΔG at $T = 25$°C, HU*Tmar* is more thermostable exhibiting a T_m near 95°C. From the data on HU*Tmar* (Ruiz-Sanz et al. 2004), such difference in thermostability cannot be attributed solely to effects for the different pH conditions. It is most likely due to the smaller values of ΔC_p obtained from fitting of the DSC profiles for HU*Tmar* (Ruiz-Sanz et al. 2004).

As it was shown by Freire's group (Hilser et al. 1997) the important contribution from structural changes upon denaturation contained in ΔG are the relative changes in the apolar and polar solvent accessible surface areas (ΔASAap and ΔASApol), as well as the distribution of interatomic distances between different atom types, which directly determine the packing density. As was pointed out earlier, based on the X-ray structure of HU*Tmar* (RCSB code: 1B8Z) and the 3D-model of the dimeric form of HU*Tvo* that was produced in this study, an apolar to polar ratio of 1.1 and 0.94, respectively, is obtained, which cannot account for the observed ΔC_p differences between the two compounds. If the structural arguments are restricted to contributions arising only from the exposure of the dimer interface, analogous results are obtained (2.9 for HU*Tmar* and 2.3 for HU*Tvo*). It can thus be concluded that the observed $\Delta G(T)$ changes between the two molecules originate from the differences in the compactness between the native and the structure-less denatured states of each protein. The values of ΔH derived for either molecule are less than what is expected for a protein of the size of HU, which, as it has already been mentioned, provides evidence that the denatured molecules of either HU*Tvo* or HU*Tmar* may still be substantially compact.

Since HU*Tvo* is in the border between archaea and eubacteria, it is anticipated that HU*Tvo* has to be more adaptable to higher temperatures compared to HU*Tmar*. Both proteins share the same fold and they are expected to follow similar mechanisms for thermal destabilization. Yet, the marine eubacterium *T. maritima* has been adapted to a less unstable environment, the marine environment and so under the influence of high pressures, differences in the compactness may arise with the HU*Tvo* fold, which is influenced by the atmospheric pressure. More HU proteins from archaea have to be studied thermodynamically in order to establish the mechanism(s) of thermal stability of such proteins from this particular kingdom.

References

Benitez-Cardoza CG, Rojo-Dominguez A, Hernandez-Arana A (2001) Temperature-induced denaturation and renaturation of triosephosphate isomerase from *Saccharomyces cerevisiae*: evidence of dimerization coupled to refolding of the thermally unfolded protein. Biochemistry 40:9049–9058

Boelens R, Vis H, Vorgias CE, Wilson KS, Kaptein R (1996) Structure and dynamics of the DNA binding protein HU from *Bacillus stearothermophilus* by NMR spectroscopy. Biopolymers 40:553–559

Bohm G, Muhr R, Jaenicke R (1992) Quantitative analysis of protein far UV circular dichroism spectra by neural networks. Protein Eng 5:191–195

Bradford M (1976) A rapid and sensitive method for the determination of microgram quantities of protein utilising the principle of protein–dye binding. Anal Biochem 72:248–254

Castaing BC, Zelwer C, Laval J, Boiteux S (1995) HU protein of *Escherichia coli* binds specifically to DNA that contains single-strand breaks or gaps. J Biol Chem 270:10291–10296

Christodoulou E, Rypniewski W, Vorgias CE (2003) High resolution X-ray structure of the DNA binding protein HU from the hyperthermophilic eubacterium *Thermotoga maritima* and the determinants of its thermostability. Extremophiles 7:111–122

Christodoulou E, Vorgias CE (2002) The thermostability of the DNA binding protein HU from mesophilic thermophilic and extreme thermophilic bacteria. Extremophiles 6:21–31

Coste F, Hervouet N, Oberto J, Zelwer C, Castaing B (1999) Crystallization and preliminary X-ray diffraction analysis of the homodimeric form alpha2 of the HU protein from *Escherichia coli*. Acta Crystallogr Biol Crystallogr D55:1952–1954

Damodaran S (2003) In situ measurement of conformational changes in proteins at liquid interfaces by circular dichroism spectroscopy. Anal Bioanal Chem 376:182–188

DeLano WL (2002) The PyMOL molecular graphics system on world wide web. http://www.pymol.org

Drlica K, Rouviere-Yaniv J (1987) Histonelike proteins of bacteria. Microbiol Rev 51:301–319

Durney MA, Wechselberger RW, Kalodimos CG, Kaptein R, Vorgias CE, Boelen R (2004) An alternate conformation of the hyperthermostable HU protein from *Thermotoga maritima* has unexpectedly high flexibility. FEBS Lett 563:49–54

Esser D, Rudolph R, Jaenicke R, Bohm G (1999) The HU protein from *Thermotoga maritima*: recombinant expression, purification and physicochemical characterization of an extremely hyperthermophilic DNA-binding protein. J Mol Biol 291:1135–1146

Futterer O, Angelov A, Liesegang H, Gottschalk G, Schleper C, Schepers B, Dock C, Antranikian G, Liebl W (2004) Genome sequence of *Picrophilus torridus* and its implications for life around pH 0. Proc Natl Acad Sci USA 101:9091–9096

Gill CS, von Hippel PH (1989) Calculation of protein extinction coefficients from amino acid sequence data. Anal Biochem 182:319–326

Gouet P, Courcelle E, Stuart DI, Metoz F (1999) ESPript: multiple sequence alignments in PostScript. Bioinformatics 15:305–308

Greenfield NJ (1996) Methods to estimate the conformation of proteins and polypeptides from circular dichroism data. Anal Biochem 235:1–10

Guex N, Peitsch MC (1997) SWISS-MODEL and the Swiss-PdbViewer: an environment for comparative protein modeling. Electrophoresis 18:2714–2723

Hilser VJ, Townsend BD, Freire E (1997) Structure-based statistical thermodynamic analysis of T4 lysozyme mutants: structural mapping of cooperative interactions. Biophys Chem 64:69–79

Hwang DS, Kornberg A (1992) Opening of the replication origin of *Escherichia coli* by DnaA protein with protein HU or IHF. J Biol Chem 267:23083–23086

Jia X, Grove A, Ivancic M, Hsu VL, Geiduscheck EP, Kearns DR (1996) Structure of the *Bacillus subtilis* phage SPO1-encoded type II DNA-binding protein TF1 in solution. J Mol Biol 263:259–268

Jones S, Thornton JM (1996) Principles of protein-protein interactions derived from structural studies. Proc Natl Acad Sci USA 93:13–20

Kamashev D, Rouvière-Yaniv J (2000) The histone-like protein HU binds specifically to DNA recombination and repair intermediates. EMBO J 23:6527–6535

Kawashima T, Amano N, Koike H, Makino S, Higuchi S, Kawashima-Ohya Y, Watanabe K, Yamazaki M, Kanehori K, Kawamoto T, Nunoshiba T, Yamamoto Y, Aramaki H, Makino K, Suzuki M (2000) Archaeal adaptation to higher temperatures revealed by genomic sequence of *Thermoplasma volcanium*. Proc Natl Acad Sci USA 97:14257–14262

Laemmli UK (1970) Cleavage of structural proteins during the assembly of the head of bacteriophage T4. Nature 227:680–685

Lavoie BD, Chaconas G (1994) A second high affinity HU binding site in the phage Mu transpososome. J Biol Chem 269:15571–15576

Lowry OH, Rosebrough NJ, Farr AL, Rendall RJ (1951) Protein measurement with the Folin phenol reagent. J Biol Chem 193:265–275

Manly SP, Matthews KS, Sturtevant JM (1985) Thermal denaturation of the core protein of lac repressor. Biochemistry 24:3842–3846

Milardi D, Rosa CL, Grasso D (1996) Theoretical basis for differential scanning calorimetric analysis of multimeric proteins. Biophys Chem 62:95–108

Oberto J, Drlica K, Rouviere-Yaniv J (1994) Histones, HMG, HU, IHF: meme combat. Biochimie 76:901–908

Pace CN, Vajdos F, Fee L, Grimsley G, Gray T (1995) How to measure and predict the molar absorption coefficient of a protein. Protein Sci 4:2411–2423

Padas PM, Wilson KS, Vorgias CE (1992) DNA binding protein from mesophilic and thermophilic *Bacilli*: cloning, overexpression and purification. Gene 117:39–44

Pettijohn DE (1988) Histone-like proteins and bacterial chromosome structure. J Biol Chem 263:12793–12796

Privalov PL, Potekhin SA (1986) Scanning microcalorimetry in studying temperature-induced changes in proteins. Methods Enzymol 131:4–51

Ramstein J, Hervouet N, Coste F, Zelwer C, Oberto J, Castaing B (2003) Evidence of a thermal unfolding dimeric intermediate for the *Escherichia coli* histone-like HU proteins: thermodynamics and structure. J Mol Biol 331:101–121

Raves ML, Doreleijers J, Vis H, Vorgias CE, Wilson KS, Kaptein R (2001) Joint refinement as a tool for thorough comparison between NMR and X-ray data and structures of HU protein. J Biomol NMR 21:235–248

Rice PA, Yang S-W, Mizuuchi K, Nash H (1996) Crystal structure of an IHF-DNA complex: a protein-induced DNA U-turn. Cell 87:1295–1306

Rouvière-Yaniv J, Yaniv M, Germond J (1979) *E. coli* DNA binding protein HU forms nucleosomelike structures with double-stranded DNA. Cell 17:265–274

Ruepp A, Graml W, Santos-Martinez ML, Koretke KK, Volker C, Mewes HW, Frishman D, Stocker S, Lupas AN, Baumeister W (2000) The genome sequence of the thermoacidophilic scavenger *Thermoplasma acidophilum*. Nature 407:508–513

Ruiz-Sanz J, Filimonov VV, Christodoulou E, Vorgias CE, Mateo PL (2004) Thermodynamic analysis of the unfolding and stability of the dimeric DNA-binding protein HU from the hyperthermophilic eubacterium *Thermotoga maritima* and its E34D mutant. Eur J Biochem 271:1497–1507

Sagi D, Friedman N, Vorgias CE, Oppenheim AB, Stavans J (2004) Modulation of DNA conformations through the formation of alternative high-order HU–DNA complexes. J Mol Biol 341:419–428

Sambrook J, Fritsch EF, Maniatis T (1989) Molecular cloning. A laboratory manual, 2nd edn. Cold Spring Harbor Laboratory Press, Cold Spring Harbor

Sanger F, Nicklen S, Coulson AR (1977) DNA sequencing with chain-terminating inhibitors. Proc Natl Acad Sci USA 74:5463–5467

Schmid MB (1990) More than just "histone-like" proteins. Cell 63:451–453

Schnurr B, Vorgias CE, Stavans J (2006) Compaction and supercoiling of single, long DNA molecules by HU protein. Bioph Rev Lett 1:29–44

Serban D, Arcineigas SF, Vorgias CE, Thomas GJ Jr (2003) Structure and dynamics of the DNA-binding protein HU of *B. stearothermophilus* investigated by Raman and ultraviolet-resonance Raman spectroscopy. Protein Sci 12:861–870

Tanaka I, Appelt K, Dijk J, White SW, Wilson KS (1984) 3-Å resolution structure of a protein with histone-like properties in prokaryotes. Nature 310:376–381

Todd MJ, Semo N, Freire E (1998) The structural stability of the HIV-1 protease. J Mol Biol 283:475–488

van Gunsteren WF, Billeter SR, Eising AA, Hünenberger PH, Krüger P, Mark AE, Scott WRP, Tironi IG (1996) Biomolecular simulation: the GROMOS96 manual and user guide. Hochschulverlag an der ETH Zürich/Biomos, Zürich/Groningen

Vis H, Mariani M, Vorgias CE, Wilson KS, Kaptein R, Boelens R (1995) Solution structure of the HU protein from *Bacillus stearothermophilus*. J Mol Biol 254:692–703

White SW, Appelt K, Wilson KS, Tanaka I (1989) A protein structural motif that bends DNA. Proteins 5:281–288

White SW, Wilson KS, Appelt K, Tanaka I (1999) The high-resolution structure of DNA-binding protein HU from *Bacillus stearothermophilus*. Acta Crystallogr D55:801–809